

# Image Reconstruction from Ipswich Data – II

*P.M. van den Berg<sup>1</sup>, B.J. Kooij<sup>1</sup>, and R. E. Kleinman<sup>2</sup>*

<sup>1</sup>Laboratory of Electromagnetic Research,  
Faculty of Electrical Engineering  
Centre for Technical Geoscience  
Delft University of Technology  
PO Box 5031  
2600 GA Delft  
The Netherlands

<sup>2</sup>Center for the Mathematics of Waves  
Department of Mathematical Sciences  
University of Delaware  
Newark, DE 19716  
USA

Keywords: Electromagnetic scattering inverse problems; image reconstruction; gradient methods

In this paper, we describe the results obtained by using variants of the modified gradient method developed earlier [1-3]. These are applied to the new Ipswich data sets to reconstruct the shape, location, and/or index of refraction of unknown two-dimensional scatterers (infinite cylinders in three dimensions). The modified gradient method was used previously in connection with two Ipswich data sets (IPS001 and IPS002). These correspond to TM polarization (the electric field polarized along the cylinder axis of the cylindrical two-dimensional scatterer), or VV in the Ipswich designation, for two perfectly conducting objects, the circular cylinder and the strip. Good reconstructions were obtained and these results were reported earlier [4]. The experimental data were re-normalized by multiplying the circular cylinder data by one unknown complex constant. This constant is determined by minimizing the  $L^2$  norm of the difference with the exact data, as computed using the representation in cylindrical wave functions. This constant, which is essentially a phase correction, was then used as a multiplier of the measured data for both the circular-cylinder data (IPS001) and the strip data (IPS002).

Subsequently, a third data set (IPS003) was set up as a “contest” for the 1995 IEEE AP-S/URSI Symposium in Newport Beach, California. It contained scattered-field data for one penetrable object, a square polystyrene cylinder [5]. However, the reconstruction could not be carried out satisfactorily, because we were not able to calibrate these data appropriately. The data sets for this penetrable case were difficult to calibrate, since they were adjusted after the Ipswich experiments in a different way than the previous ones, for the conducting cases. After the shape and index of refraction of this object became known, we re-normalized the IPS003 data by multiplying the data with one complex constant that is determined by minimizing the  $L^2$  norm of the difference with numerically computed data, and we reconstructed the square polystyrene very well. We presented these results at the 1996 IEEE AP-S/URSI Symposium in Baltimore, Maryland. We will not present these results in this paper, since this paper is devoted to the new data sets, which were the subject of the “contest” at the 1996 IEEE AP-S/URSI Symposium, viz., the reconstruction of the data sets IPS004, IPS005, IPS006, IPS007, and IPS008. Reconstruc-

tions using these data sets with the modified gradient method will be reported.

The modified gradient was introduced in [1, 2], for the reconstruction of the complex relative permittivity of inhomogeneous scatterers. Very briefly, the method is described as follows. An unknown inhomogeneity,  $B$ , imbedded in free space, is illuminated successively by a number of incident fields,  $u_j^{inc}$ ,  $j=1,2,\dots,J$ , at the same frequency, but originating in different places (different line sources, or plane waves with different angles of incidence). In the case of the new Ipswich experiments, we have 36 angles of incidence, equidistantly distributed around the object. The unknown scatterer is assumed to be located somewhere in a known, bounded, test domain,  $D$  (taken to be a square), and the scattered field is measured on a domain  $S$  (taken to be circle), containing the test domain,  $D$ , in its interior. In the case of the new Ipswich experiments,  $S$  was taken to be in the far zone of the scattered field at 18 angles of observation equidistantly distributed over a semi-circle. For each experiment, this semi-circle starts with the forward-scattering angle.

Rather than working with the complex relative permittivity, we introduce the complex contrast

$$\chi = \varepsilon/\varepsilon_0 - 1 + i\sigma/\omega\varepsilon_0. \quad (1)$$

For each incident field,  $u_j^{inc}$ , the total field is denoted by  $u_j$ . The total fields,  $u_j$ , and the contrast,  $\chi$ , have to satisfy a domain integral equation in  $D$  (the object equation), and an integral representation for the scattered field in  $S$  (the data equation). The modified gradient method consists of constructing sequences of approximations to  $u_j$  and  $\chi$ , starting from initial estimates,  $u_{j,0}$  and  $\chi_{j,0}$ , as follows:

$$u_{j,n} = u_{j,n-1} + \alpha_n v_{j,n}, \quad \chi_n = \chi_{n-1} + \beta_n d_n, \quad (2)$$

where  $\alpha_n$  and  $\beta_n$  are constants, and the update directions,  $v_{j,n}$  and  $d_n$ , are functions on  $D$ . Since these updates for the total field and the contrast do not satisfy the object and data equations, we introduce two error measures,  $r_{j,n}$  and  $\rho_{j,n}$ . These are defined on  $D$  and  $S$ , respectively, as

$$r_{j,n} = u_j^{inc} - u_{j,n} + G_D \chi_n u_{j,n}, \quad \rho_{j,n} = f_j - G_S \chi_n u_{j,n}, \quad (3)$$

where  $f_j$  denotes the measured scattered field on  $S$ , and where  $G_D$  and  $G_S$  are integral operators [2], operating on  $\chi_n u_{j,n}$ . The constants  $\alpha_n$  and  $\beta_n$  are determined by minimizing the value of the cost functional

$$F_n = \frac{\sum_{j=1}^J \|r_{j,n}\|_D^2}{\sum_{j=1}^J \|u_j^{inc}\|_D^2} + \frac{\sum_{j=1}^J \|\rho_{j,n}\|_S^2}{\sum_{j=1}^J \|f_j\|_S^2}, \quad (4)$$

where  $\|\cdot\|_D$  and  $\|\cdot\|_S$  denote the  $L^2$  norms on  $D$  and  $S$ , respectively. The update directions,  $v_{j,n}$  and  $\chi_n$ , are chosen as the Polak-Ribière conjugate-gradient directions of the cost functional with respect to the field, assuming that  $\chi = \chi_{n-1}$ , and with respect to the contrast, assuming that  $u_j = u_{j,n-1}$  [2]. The initial estimates,  $u_{j,0}$  and  $\chi_0$ , are obtained by a back-propagation of the measured data, as described in [3].

The algorithm outlined above was changed somewhat, to incorporate a priori information about the Ipswich objects. For the perfectly conducting objects, the contrast was assumed to be positive imaginary. This was ensured in the algorithm by replacing  $\chi_n$  by  $i\zeta_n^2$ , and updating the contrast by the relation  $\zeta_n = \zeta_{n-1} + \beta_n \xi_n$ , where  $\zeta_n$ ,  $\beta_n$ , and  $\xi_n$  are real. This is described in [3], and was employed in connection with the circular-cylinder data (IPS001) and the strip data (IPS002), which were, at the time, mystery targets, as detailed in [4]. For penetrable objects, we assume the contrast to be positive real. This was ensured in the algorithm by replacing  $\chi_n$  by  $\zeta_n^2$ , with accompanying changes in the update directions and initial estimates. This was used in [5], in connection with the data of the square polystyrene cylinder (IPS003).

The new Ipswich data sets (IPS004-IPS008) are all given in the same form, and a perfectly conducting circular-cylinder data set

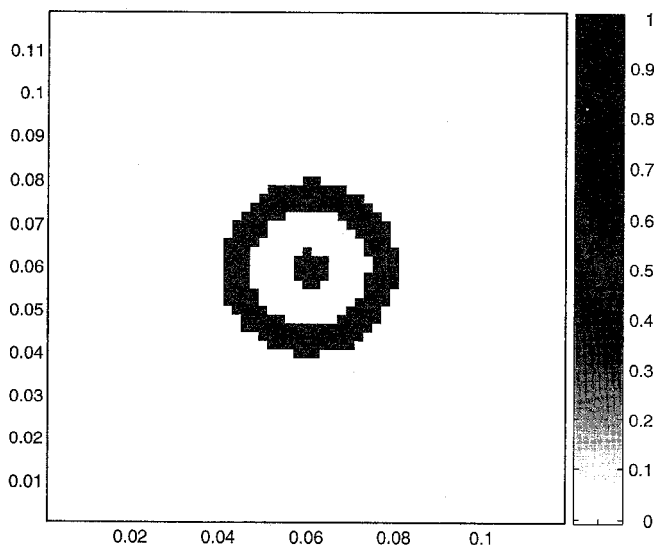


Figure 1. The reconstruction of the aluminum circular cylinder (IPS006).

(IPS006) was also given, which enables a consistent re-normalization to obtain a phase correction and a slight amplitude correction. From the latter data set, we observe that the circular cylinder is not located exactly at the origin of the coordinate system. Hence, we can only compare the forward-scattering data,  $f_j^{exp}$ , with the analytical data,  $f_j^{anl}$ . A complex correction factor,  $\gamma$ , was found by

defining  $\gamma$  to be the minimizer of  $\sum_{j=1}^J |f_j^{anl} - \gamma f_j^{exp}|^2$ . We found that

$$\left( \frac{\sum_{j=1}^J |f_j^{anl} - \gamma f_j^{exp}|^2}{\sum_{j=1}^J |f_j^{anl}|^2} \right)^{1/2} = 0.04. \quad (5)$$

The correction factor,  $\gamma$ , was then used to modify the measured data of the new Ipswich data sets in a similar way as in [4, 5]. Using these recalibrated data, we ran the inversion algorithm.

## 1. IPS006

We first present the reconstructed image of the Ipswich data set, IPS006, the known perfectly conducting circular cylinder with radius of 15.9 cm. We took a test domain,  $D$ , with sides of 12 cm, or  $4\lambda$ , since the wavelength,  $\lambda$ , in all experiments was 3 cm. The test domain was subdivided into  $60 \times 60$  subsquares for the computations, and the imaginary value of the contrast after 64 iterations is depicted in Figure 1. As described in [3, 4], the reconstruction of a boundary was aided considerably if an upper limit was placed on the contrast. We took the maximum amplitude of the contrast to be one. In this way, we also ensured that the mesh size was always less than one-tenth of the internal wavelength. This is necessary for an accurate computation of the field values. After 32 iterations, the image did not improve anymore, and we terminated the scheme after 64 iterations with a cost functional of  $F_{64}^{1/2} = 0.13$ .

## 2. IPS004

Observing that our reconstruction of the circular cylinder was successful, we continued to reconstruct the perfectly conducting object from the data set IPS004, the aluminum dihedral. However, this corresponds to TE polarization (the electric field polarized transverse to the cylinder axis), or HH in the Ipswich designation. But the problem is that no experimental data with respect to the TE scattering from a circular cylinder had been supplied, so that no proper calibration of the data could be carried out. Secondly, the object and data equations for the TE case require a different approach, which is not appropriate to outline here. Thirdly, the present object was known and, hence, did not really fit in the "contest." Although we have implemented the modified gradient method for this case, and we guessed that for the TE polarization we have to multiply the data with an extra imaginary factor  $-i$ , and although we presented these results at the Baltimore Symposium, in view of the reasons above, we do not present them here.

## 3. IPS005

We now continue with the first mystery object (IPS005), with a priori information that the object is penetrable and lies inside a

circle of radius of 15 cm. We assumed that the contrast was real and positive. We took a test domain,  $D$ , with sides of 30 cm, or  $10\lambda$ . The test domain was taken to be subdivided into  $60 \times 60$  subsquares. The maximum amplitude of the contrast was taken to be one. Then, the mesh size was always less than about one fifth of the internal wavelength. This is really the upper limit for an adequate computation of the field values. After 64 iterations, the image did not improve significantly, and we terminated the scheme after 128 iterations, with a cost functional of  $F_{128}^{1/2} = 0.07$ . The reconstruction results of the real values of the contrast are depicted in Figure 2. From this we clearly observe a dihedral-shaped object, with a permittivity of about 2.

#### 4. IPS007

We now continue with the second mystery object (IPS007), with a priori information that the object is penetrable and lies

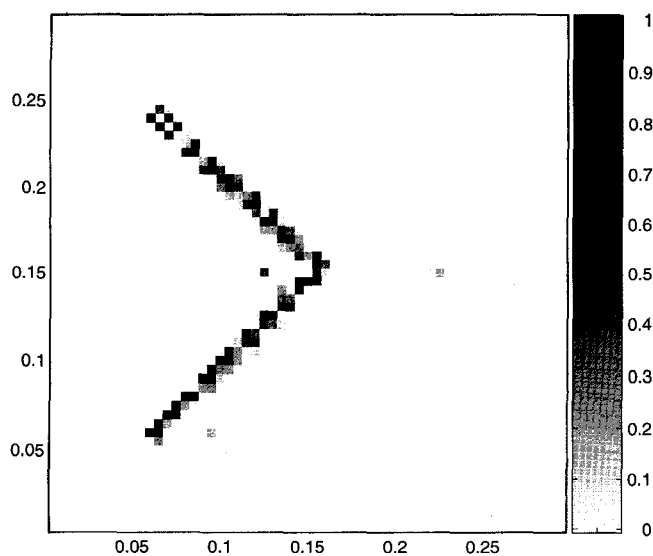


Figure 2. The reconstruction of the mystery object IPS005.

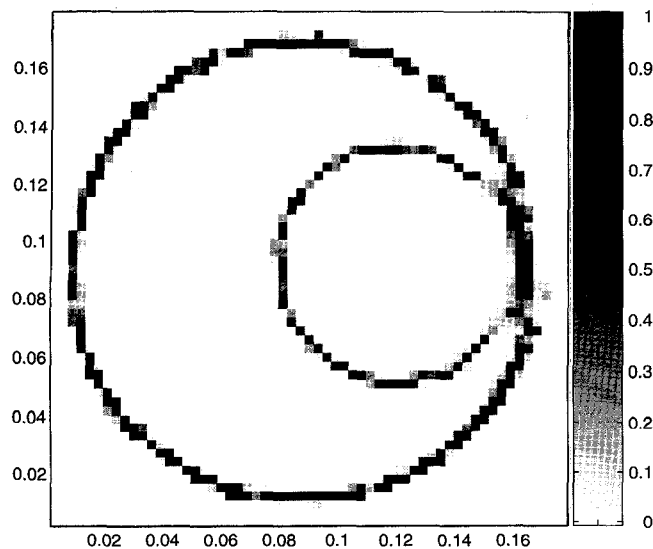


Figure 3. The reconstruction of the mystery object IPS007.

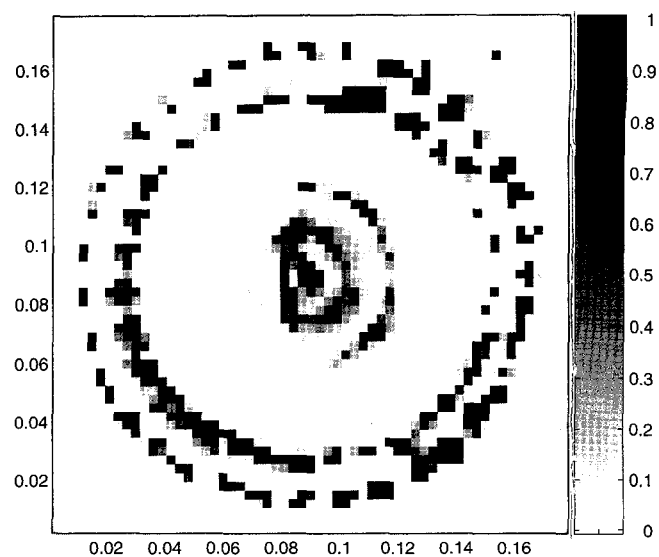


Figure 4. The reconstruction of the mystery object IPS008.

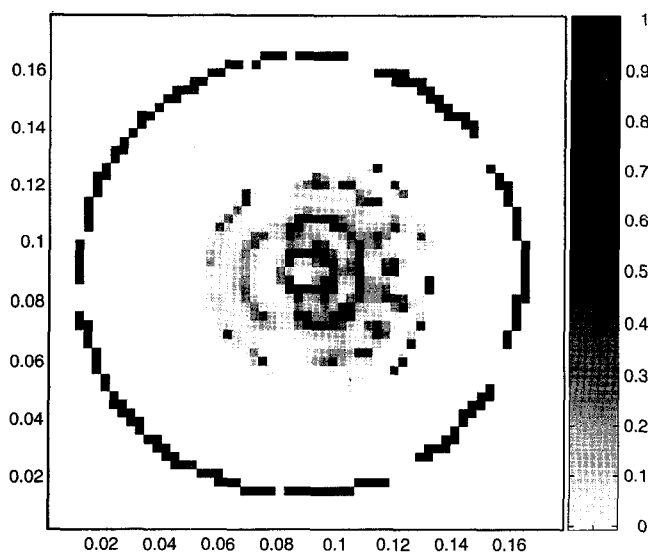


Figure 5. The reconstruction of the mystery object IPS008, using reciprocity.

inside a circle of radius of 7.5 cm. We assumed that the contrast is real and positive. We took a test domain,  $D$ , with sides of 18 cm, or  $6\lambda$ . The test domain was taken to be subdivided into  $60 \times 60$  subsquares. The maximum amplitude of the contrast was taken to be one. Then, the mesh size was always less than about one-seventh of the internal wavelength. After 64 iterations, the image did not improve significantly, and we terminated the scheme after 128 iterations, with a cost functional of  $F_{128}^{1/2} = 0.07$ . The reconstruction results of the real values of the contrast are depicted in Figure 3. The present object was clearly a circular tube, with a smaller one in its interior, both having a permittivity of about 2.

#### 5. IPS008

For the third and last mystery object (IPS008), we had the a priori information that the object is penetrable and lies inside a cir-

cle of radius of 7.5 cm. We assumed that the contrast was real and positive. The test domain and subdivision was taken to be the same as in the previous case. We observed that the cost function did not decrease substantially as a function of the number of iterations. After 128 iterations, its value was still very large:  $F_{128}^{1/2} = 0.16$ . The reconstruction results of the real values of the contrast are depicted in Figure 4, but we were pretty sure that these results were not reliable. We therefore applied reciprocity to complete the data, except for the back-scattering data. Instead of  $36 \times 18$  data points, we then had  $36 \times 35$  data points. The reconstruction results are depicted in Figure 5. The outside boundary seems to be reconstructed well. It seems to be the outer tube of the previous case, but inside we did not trust the results, since the cost functional with respect to the increased number of data points was still too large:  $F_{128}^{1/2} = 0.22$ . The reasons for the present failure of proper reconstruction may be found in the observations that we may need more data points to reconstruct the interior, and that the assumption of real contrast does not hold. After the composition of this mystery object was revealed, it seems that the latter assumption may be violated.

Judgments of the power and robustness of the modified gradient method for reconstructing the shape and the index of refraction of an inhomogeneous object are left to the reader.

## 6. Acknowledgment

This work was supported under AFOSR Grant No. F49620-96-1-0039.

## 7. References

1. R. E. Kleinman and P. M. van den Berg, "A Modified Gradient Method for Two-Dimensional Problems in Tomography," *Journal of Computational and Applied Mathematics*, **42**, 1992, pp. 17-35.
2. R. E. Kleinman and P. M. van den Berg, "An Extended Range Modified Gradient Technique for Profile Inversion," *Radio Science*, **28**, 1993, pp. 877-884.
3. R. E. Kleinman and P. M. van den Berg, "Two-Dimensional Location and Shape Reconstruction," *Radio Science*, **29**, 1994, pp. 1157-1169.
4. P. M. van den Berg, M. G. Coté, and R. E. Kleinman, "Blind Shape Reconstruction from Experimental Data," *IEEE Transactions on Antennas and Propagation*, **AP-43**, 1995, pp. 1389-1396.
5. P. M. van den Berg and R. E. Kleinman, "Image Reconstruction from Ipswich Data," *IEEE Antennas and Propagation Magazine*, **38**, pp. 56-59. ☞



## Editor's Comments *Continued from page 5*

tional methods. I believe the GA is going to play an important role in antenna-design methodology, and this article does an excellent job of showing how it can be used.

Not quite a year ago, Dick Dowden and colleagues described the red-sprite phenomenon, and what was known about it based on VLF-scatter measurements, in an article in this *Magazine*. In Dick's article with Craig Rodger, in this issue, the authors explore what can be determined about the structure and physical param-

eters of the sprites, using a simple model. This article is fascinating from at least two standpoints. First, it provides some rather good limits on the possible values that can be associated with the sprite plasma. Even if you are not someone with a keen interest in radio propagation in magneto-plasmas, you'll find this article both interesting, and readily understandable. In part, that's because of the second aspect: The authors do an excellent job of using a simple model, and the basic physics of the scattering involved, to arrive at a surprisingly rich set of results. This article is worth reading just to enjoy the physical reasoning and adept modeling employed.

The Parkes 60 m radio telescope is one of the world's great radio astronomy observing instruments. It also is a very interesting, very large antenna. Bruce Thomas and his colleagues have given us an exciting look at what is involved in a major upgrade to such a facility. What I found fascinating about this work was the complex interrelationships among the various components and subsystems in the facility. As always in such large instruments, the mechanical aspects must be considered as an integral part of the engineering, along with the electromagnetic performance. This article is enjoyable reading, both because of the way in which it is written, and because of the glimpse into the elegant complexity of such instruments.

The challenge of reconstructing an image of an unknown scatterer from electromagnetic fields scattered by it is a problem that almost everyone in electromagnetics has thought about, at some time or another. I think part of the breadth of appeal of such inverse problems is that many of us have this intuitive feeling that such problems shouldn't be that difficult to solve. In turn, I think that's because so much of our learning process is tied up with our vision system, and mental visualization. We do this kind of image reconstruction almost every waking moment, and even when we dream, at optical wavelengths. Why should making the wavelength longer and the radiation coherent make the problem so much harder? Well, it does, and part of the reason is because while we do not have to understand visible-light scattering in order to see, we do have to understand and be able to properly process longer-wavelength scattering in order to reconstruct an image we can see. That understanding and processing is the topic of the Special Session on Image Reconstruction Using Real Data. For the second year in a row, we have a set of selected mini-articles from that special session, held at the Baltimore AP-S/URSI Symposium. What sets these special sessions apart, among other things, is that all of the presentations deal with the same data set: the Ipswich data. These are *measured* data, collected at the US Air Force Ipswich Measurement Facility. They involve a variety of targets, some of which were known to the authors before the session, and some of which were not. The result is a fun and fascinating look at how a variety of techniques perform on the same sets of data. Robert McGahan and Ralph Kleinman have served as "guest Editors" in assembling these mini-articles, and have written the introduction to the set, as well. The results are getting better each year. It will be interesting to see what happens at the Montreal Symposium's special session. One added note: In addition to the description of the targets and the data sets given in the introductory article, the article by J. B. Morris, R. V. McGahan, J. L. Schmitz, R. M. Wing, D. A. Pommet, and M. A. Fiddy gives additional information on the data sets. It also shows how what has now become an almost "classic" inverse technique—back-propagation, using aspect diversity in diffraction tomography—performs on each data set.

I must correct one comment I made in this column in the last issue. Simon Walker's article, in the February issue, did not con-

*Continued on page 85*